

## Automatic Bolus Analysis for DCE-MRI Using Radial Golden-Angle Stack-of-stars GRE Imaging

Robert Grimm<sup>1</sup>, Li Feng<sup>2</sup>, Christoph Forman<sup>1</sup>, Jana Hutter<sup>1</sup>, Berthold Kiefer<sup>3</sup>, Joachim Hornegger<sup>1</sup>, and Tobias Block<sup>2</sup>

<sup>1</sup>Pattern Recognition Lab, FAU Erlangen-Nuremberg, Erlangen, Germany, <sup>2</sup>Department of Radiology, NYU Langone Medical Center, New York City, NY, United States, <sup>3</sup>Siemens Healthcare, Erlangen, Germany

**INTRODUCTION:** In clinical 3D Dynamic Contrast-Enhanced MRI (DCE-MRI) of the abdomen, multiple phases of perfusion (pre-contrast, arterial, venous, delayed phases) are captured subsequently in breath-hold scans. Novel imaging and reconstruction techniques such as GRASP<sup>1</sup> promise DCE-MRI at a temporal resolution of only few seconds from a single, continuous image acquisition. This reduces the requirements on bolus-timing accuracy and can thereby significantly simplify the imaging workflow. However, the technique also has two disadvantages that have not been addressed so far: First, it cannot be combined with conventional bolus detection techniques<sup>2,3</sup> to monitor the contrast agent (CA) bolus. Because the reconstruction is computationally so intensive that dynamic images are computed with significant delay, no direct visual feedback is available after the scan. Second, the resulting 4D images that can comprise more than 100 time-steps<sup>4</sup> impose a significant amount of data that cannot yet be adequately visualized or analyzed with most clinical imaging software. Identifying the few critical phases of perfusion in the time series requires manual interaction from the radiologist, or carefully tuned, application-specific segmentation algorithms<sup>5</sup>. Here, we propose a parameter-free method to automatically extract a bolus time curve from raw k-space data acquired with a radial stack-of-stars GRE sequence. It can be used to display statistics about the CA bolus right after the scan, as well as to automatically pick time frames at important stages of perfusion. Because the approach is k-space-based, the temporal accuracy is not limited by the reconstructed images.

**THEORY:** The method is closely related to respiratory self-gating techniques that have been proposed for MRI with radial k-space trajectories<sup>6,7</sup>. The course of contrast enhancement causes an increase in the total transverse magnetization, which is reflected in the magnitude of the central samples of every radial spoke in the k-space center partition ( $k_z = 0$ ). With this technique, a 1D signal can be extracted for every acquired channel. PCA compression<sup>8</sup> is then applied to reduce the multi-channel data to a single 1D signal. The typical time course of enhancement in a volume is a constant section before CA injection, followed by a rapid signal increase at bolus arrival and a slow wash-out. These three phases are modeled using a constant, a linear, and another constant line segment. This model requires only two degrees of freedom, referred to as  $x_1$  and  $x_2$  in the following. The pre-contrast segment ends at time point  $x_1$  while the washout begins at  $x_2$ . The model is fitted by exhaustive search using the following cost function:

$$f(x_1, x_2) = \sum_{i=1}^{x_1} (B_i - y_1(x_1))^2 + \sum_{i=x_1+1}^{x_2-1} \left( B_i - \frac{y_2(x_2) - y_1(x_1)}{x_2 - x_1} \cdot (i - x_1) - y_1(x_1) \right)^2 + \sum_{i=x_2}^N (B_i - y_2(x_2))^2,$$

where  $B_i$  is the  $i$ -th sample in the enhancement signal  $\mathbf{B}$  of length  $N$ , and  $y_1(x_1)$  and  $y_2(x_2)$  are the values obtained by least-squares fitting of a constant line segment to the first  $x_1$  (or last  $N - x_2 + 1$ ) samples of the enhancement signal.

The ratio of the distance between the constant segments to the standard deviation of the signal during the whole acquisition,  $(y_2 - y_1) / \text{std}(\mathbf{B})$ , can be used as a simple indicator of actual contrast enhancement. The onset time  $x_1$  and plateau time  $x_2$  provide additional checks whether the bolus arrival was truly captured by the acquisition. After image reconstruction, the critical phases of perfusion can be found by using population-based estimates for the respective delays from the detected bolus time  $x_1$ .

**METHODS:** To evaluate the proposed method, four IRB-approved pediatric studies were analyzed retrospectively. All scans were performed on a 1.5 T MAGNETOM Avanto scanner (Siemens Healthcare, Erlangen, Germany) with a radial stack-of-stars 3D GRE sequence and during free breathing. The scan time was 193-275 s for 800 radial spokes with a base resolution of 256 pixels and 96-144 slices. The bolus signal was extracted and  $x_1$  and  $x_2$  were computed as described above. All datasets were reconstructed using GRASP with 13 radial spokes per time-step, corresponding to an average temporal resolution of 3.6 +/- 0.6 s. The relevant key phases were determined manually using a single slice through the liver and kidneys. For the enhancement onset and optimal arterial phase as defined by Sharma et al.<sup>2</sup>, only single time points were picked. The range of time steps depicting the venous enhancement was characterized by a time window. The average delays of the arterial image and the middle of the venous phase with respect to  $x_1$  were used to select the key images from the reconstructed dataset. The pre-contrast image was selected in the center of the pre-contrast section.

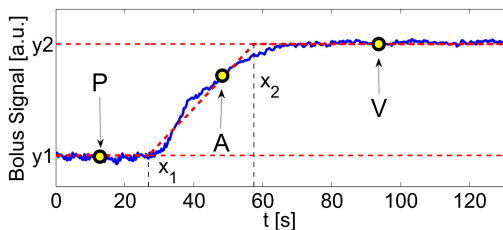


Fig. 1: Bolus signal (blue) and fitted model (dashed red). Fig. 2: Automatically selected pre-contrast (P), arterial (A), and venous (V) phase images.

**RESULTS AND DISCUSSION:** Automatic bolus detection succeeded in all examined datasets. Fig. 1 shows the derived volume enhancement curve as well as the fitted model for one of the datasets. The average distance between  $y_1$  and  $y_2$  was 3.0 +/- 0.45 standard deviations of  $\mathbf{B}$ , indicating clearly separated phases and, hence, successful bolus administration in all cases. Between 8.3 and 32.2 s of raw data were acquired before bolus arrival, permitting sufficient image quality again in all datasets. The average duration of the detected enhancement phase was 28.9 +/- 3.9 s.

The average delay between detected onset and arterial phase was 20.5 +/- 1.5 s, while the average delay between onset and venous phase was 65 +/- 8.4 s. The time frame for good venous contrast spanned between 25 and 32 s. The average error between automatically detected bolus arrival  $x_1$  and the manually labeled onset was 1.9 +/- 1.2 s, which was in all cases within the temporal resolution of the reconstructed images. Using the estimated constant offsets, the average error between the projected time point for the arterial/venous phase and the reference labels was 1.2 +/- 0.7 s and 6.2 +/- 4.5 s, respectively. The correctness of the images could be confirmed visually, as shown in Fig. 2: No enhancement in the pre-contrast image, maximal enhancement of the portal vein but no enhancement of hepatic veins in the arterial phase, and enhancement of all vessels in the venous phase.

**CONCLUSION:** The proposed method allows fully automatic extraction of a signal characterizing the course of contrast enhancement in golden-angle radial DCE-MRI acquisitions. Fitting a three-segment model is used to precisely detect the bolus arrival, making it possible to immediately recognize cases where the bolus administration failed. Using population-based estimates for the delay of arterial and venous phases of perfusion, the detected bolus onset can be used to automatically extract the clinically relevant key images from a dynamic time series. Future work will focus on validating the method in larger patient studies and on deriving the optimal phases of perfusion from the bolus signal rather than using constant offsets.

### REFERENCES:

- [1] Feng et al. #0081, ISMRM 2012.
- [2] Sharma et al. JMRI 33, p. 110, 2011.
- [3] Hussain et al. Radiology 226, 2003.
- [4] Kim et al. #1468, ISMRM 2012.
- [5] Chen et al. LNCS 5241, p. 594, 2008.
- [6] Lin et al. MRM 60, p. 1135, 2008.
- [7] Grimm et al. #0598, ISMRM 2012.
- [8] Buehrer et al. MRM 57, p. 1131, 2007.